

# Interrelation between the thermodynamic and viscometric behaviour of aqueous solutions of hydrophobically modified ethyl hydroxyethyl cellulose

M.V. Badiger, A. Lutz, B.A. Wolf\*

*Institut für Physikalische Chemie, Johannes Gutenberg-Universität, Jakob-Welder-Weg 13, D-55099 Mainz, Germany*

Received 8 March 1999; accepted 8 April 1999

---

## Abstract

Aqueous solutions of a commercial sample of hydrophobically modified ethyl hydroxyethyl cellulose (HC,  $M_w = 100$  kg/mol, nonylphenol substitution ca. 1.7 mol%) were studied with respect to their demixing behaviour and flow characteristics. Phase separation temperatures were measured turbidimetrically and by determining the first discernible macroscopic phase separation. In some cases demixing was also monitored viscometrically. Phase volume ratios yielded a critical polymer concentration of 1.87 wt.% HC (displaced considerably out of the minimum of the demixing curve towards higher polymer concentrations) and a lower critical solution temperature of 47°C. Model calculations of the spinodal curve indicate a moderately exothermal heat of mixing. This conclusion is backed by the intrinsic viscosities determined from 25 to 55°C. In this  $T$ -range  $[\eta]$  falls in a sigmoidal manner to approximately one fourth of its value at the lowest temperature (430 ml/g). In spite of short, stiff chains and high dilution (max. 2.5 wt.% HC) these liquids have a highly developed tendency of shear thinning. Further, they exhibit an uncommonly large critical excess viscosity and the dependencies of the zero shear viscosities on composition and temperature show several peculiarities. All these findings and the observed shear induced expansion of the homogenous region by more than 5°C are explained consistently in terms of long-lived clusters between the hydrophobic entities of HC established under equilibrium conditions. © 1999 Elsevier Science Ltd. All rights reserved.

*Keywords:* Hydrophobically modified ethyl hydroxyethyl cellulose; Aqueous solutions; Phase diagram

---

## 1. Introduction

Hydrophobically modified polymers are attracting increasing attention because of their unusual rheological properties and potential industrial applications. Such materials can, for example, be used as improved rheological modifiers in water based paint formulations, as cosmetic lotions, skin care products and in enhanced oil recovery [1,2]. In view of this practical utilisation it appears essential to understand the physico-chemical behaviour of these products in aqueous solution.

In the present study we have measured the equilibrium phase diagram of the system water/hydrophobically modified ethyl hydroxyethyl cellulose [HC] and performed some orienting experiments concerning the influence of shear on

the demixing conditions. Viscosities as a function of composition, temperature and shear rate were determined and interpreted on the basis of this thermodynamic information.

## 2. Experimental

HC was obtained from Akzo Nobel AB, Stenungsund, Sweden. This product is commercially known as Bermocoll EHM-100. The chemical structure of the polymer is given in Fig. 1.

According to the supplier each anhydroglycose unit bears an average of 1.8 hydroxyethyl groups and 60–70% of these anhydroglycose units carry a ethyl group. According to the literature [3] the hydrophobic modification of HC consists in a nonylphenol substitution of ca. 1.7 mol% and the molecular weight of the polymer is reported to be 100 kg/mol. Before its use, the polymer was purified as described in the literature [3].

---

\*Corresponding author. Tel.: +49-6131-39-2491; fax: +49-6131-39-4640.

*E-mail address:* bernhard.wolf@uni-mainz.de (B.A. Wolf)



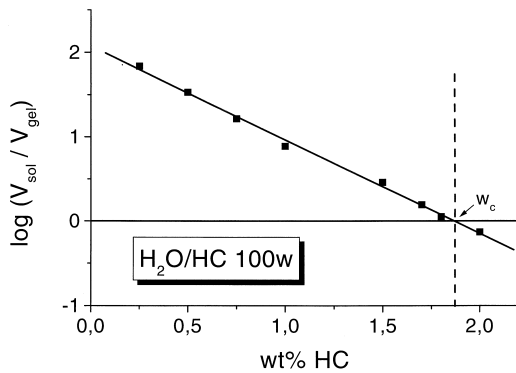


Fig. 3. Concentration dependence of  $\log(V_{\text{sol}}/V_{\text{gel}})$  for the system  $\text{H}_2\text{O}/\text{HM EHEC 100w}$  and the first sizeable macroscopic phase separation;  $V_{\text{sol}}$  and  $V_{\text{gel}}$  are the volumes of the polymer lean and the polymer rich phase, respectively. At the critical composition  $V_{\text{sol}}$  and  $V_{\text{gel}}$  become identical.

graduated cylindrical tubes of 0.8 cm diameter and 18 cm height.

### 2.2. Capillary viscometry

For dilute solutions (polymer concentration up to 1.5 wt.%) viscosities were measured as function of temperature using Ubbelohde-type capillary viscometers [6]. Relative viscosities  $\eta_{\text{rel}} = \eta_{\text{solution}}/\eta_{\text{H}_2\text{O}}$  were calculated from the flow times. Maximum shear rates varied from 0.01 to  $0.2 \text{ s}^{-1}$ .

### 2.3. Rotational viscometry

Steady state shear viscosities were measured on a shear controlled rheometer, (CV-100, Haake, Karlsruhe, Germany) as a function of temperature (typically from 20 to  $60^\circ\text{C}$ ) and shear rate  $\dot{\gamma}$  (between 1.0 and  $300 \text{ s}^{-1}$ ) using a concentric cylinder geometry (gap 1.09 mm, inner and outer radii of 6.955 and 7.500 mm, respectively). The temperature was typically varied at a rate of  $0.5^\circ\text{C}/\text{min}$  by means of a Haake thermostat interfaced with a computer. Spreading a thin layer of oil (Wacker Silicone oil) on the surface of the

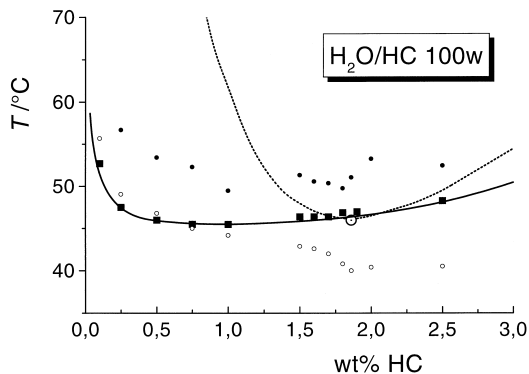


Fig. 4. Phase diagram of the system  $\text{H}_2\text{O}/\text{HC 100w}$ . Full squares: first sizeable coexistence of two phases, big circle: critical point, small circles:  $T_1$  (open) and  $T_2$  (full). Also indicated is the spinodal line calculated on the basis of Eq. (3) for  $A = 0.42$  and  $B = 310^{-4} \text{ K}^{-1}$ .

solution minimised the evaporation of solvent during the measurements.

## 3. Results and discussion

### 3.1. Thermodynamic behaviour

In order to obtain a more detailed picture of phase separation, we have in addition to cloud point temperatures ( $T_1$  and  $T_2$ ) and phase separation temperature  $T_{\text{tp}}$  also determined the critical composition of the system. This information was obtained by means of the volume ratios of the first sizeable coexisting phases; the evaluation of these data [5] is shown in Fig. 3.

All thermodynamic results are shown in Fig. 4. A comparison of the actual demixing conditions, i.e. the real macroscopic coexistence of two phases, with the turbidimetric data  $T_1$  and  $T_2$  demonstrates the uncertainty of the latter information. For very low polymer concentrations a second phase is already segregated before the system becomes significantly cloudy. On an increase in concentration one passes a region within which  $T_1$  coincides reasonably well with the demixing conditions. Thereafter, at near critical concentrations, the occurrence of critical opalescence leads to turbid solutions, which are still homogeneous, which means that the phase separation conditions correspond to very turbid solutions. Another feature that can be seen from the phase diagram of Fig. 4 is the shift of the critical composition out of the extremum of the demixing curve towards higher polymer concentration which is typical for molecularly uniform samples [7].

For a better understanding of the thermodynamic behaviour of the system, we have also performed some model calculations in terms of the Flory–Huggins equation [8]

$$\Delta G = RT\{n_1 \ln \varphi_1 + n_2 \ln \varphi_2 + gn_1 \varphi_2\}, \quad (1)$$

where the Gibbs energy of mixing,  $\Delta G$ , is given by  $n_i$ , the number of moles of the components  $i$ ,  $\varphi_i$ , their volume fraction, and the specific interactions quantified by the interaction parameter,  $g$ . The LCSTs observed with such systems are generally interpreted as a consequence of unfavourable entropic contributions due to hydrophobic association, which get more important with temperature increase.

In terms of  $g$  this situation is described [9] as

$$g = \frac{\alpha}{T} + \beta T. \quad (2)$$

Eq. (2) was therefore used first to model the spinodal line of the present system. To that end, we calculated the equivalent number of polymer segments from the known critical composition and therefrom  $g_c$ , the critical value of the interaction parameter relevant to the critical temperature  $T_c$ . Eq. (2) then yields an interrelation between  $\alpha$  and  $\beta$  which must be fulfilled to fix the minimum of the spinodal curve at the critical point. After that the two parameters were varied conjointly until a spinodal was found which is

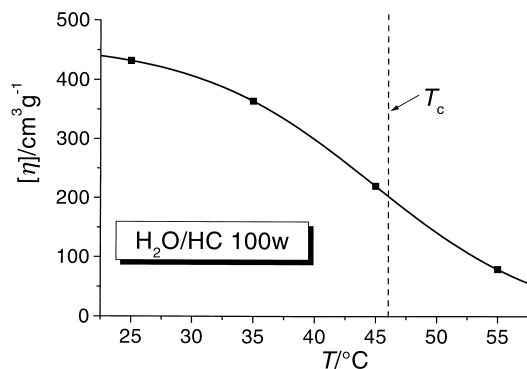


Fig. 5. Temperature dependence of the intrinsic viscosity of HC in water; the critical temperature is indicated by the broken vertical line.

situated well inside the demixing curve and agrees in its shape with theoretical expectation. Despite the fact that Eq. (2) can meet this condition well, it turned out inappropriate for the present system since it implies the occurrence of an endothermal critical temperature immediately below the present exothermal  $T_c$ , in contrast to the experimental observations according to which the solutions remain homogeneous down to the freezing point of water.

For that reason Eq. (2) was substituted by the following relation which does not model a change in the heat of mixing upon a variation of temperature

$$g = A + BT. \quad (3)$$

The spinodal curve shown in Fig. 4 results for  $A = 0.42$  and  $B = 310^{-4} \text{ K}^{-1}$  and corresponds to a moderately exothermal system. According to that temperature dependence of  $g$ , the solvent quality should slowly improve upon cooling until theta conditions would be reached at  $-17^\circ\text{C}$ . This result is not only consistent with the observed phase behaviour but also with the thermodynamic effects on the viscosity noticed with the present polymer/solvent system as demonstrated in the next section.

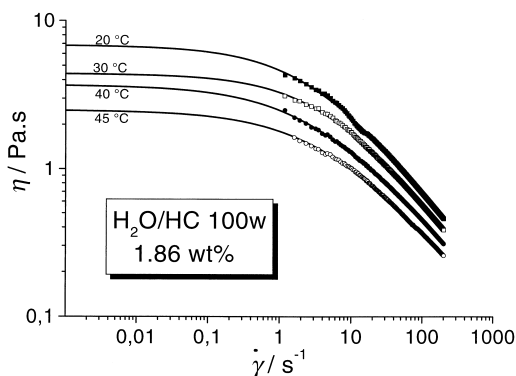


Fig. 6. Shear rate dependence of the viscosity for a 1.86 wt.% aqueous solution of HC at the different indicated temperatures. The curves are calculated according to Eq. (5).

### 3.2. Intrinsic viscosities

One viscometric quantity that reflects the thermodynamic properties of a solvent in a rather clear-cut manner is the intrinsic viscosity  $[\eta]$ , i.e. the hydrodynamic specific volume of an isolated polymer coil. The viscosity of the solutions,  $\eta$ , and that of the solvent,  $\eta_s$ , were measured as a function of polymer concentration  $c_2$  by means of capillary viscometry and evaluated with respect to  $[\eta]$  according to Schulz–Blaschke [10].

$$\frac{\eta - \eta_s}{c_2 \eta_s} = [\eta] \left( 1 + k_{SB} \frac{\eta - \eta_s}{\eta_s} \right). \quad (4)$$

The temperature dependence of the intrinsic viscosity, displayed in Fig. 5, does not exhibit a maximum; there is no indication of a change in the heat of mixing. The polymer molecules are considerably expanded at low  $T$  and shrink upon heating by a factor of almost five. This behaviour is due to an increasing extent of intramolecular clustering of segments, resulting from the decreasing solvent power, and can be followed beyond  $T_c$  as long as the dilute solutions required for the determination of  $[\eta]$  remain homogeneous. In agreement with the experimental experience this reduction in the intrinsic viscosities corresponds to an increase in the intermolecular hydrodynamic interaction as discernible in  $k_{SB}$  [11]. It is worthwhile to mention that this parameter results abnormally high for the present polymer and increases from 3.6 to 7.3 as  $T$  is raised.

### 3.3. Flow curves

Aqueous solutions of HC become shear thinning within the normally applied shear rates, which are already at high dilution despite the comparatively low molar mass  $M$  of this polymer. For instance, for 1 wt.% and at  $25^\circ\text{C}$  this effect sets in at approximately  $10 \text{ s}^{-1}$ . In view of the low  $M$ , pronounced chain stiffness and high dilution this behaviour cannot be attributed to entanglements. This assessment is supported by the shape of the shear rate dependent  $\eta$ , which cannot be described along the usual lines. Such curves, Fig. 6 gives an example for a solution with critical composition and different temperatures, were therefore represented by the following empirical formula [12]

$$\eta = \frac{\eta_0}{(1 + k \dot{\gamma}^n)}, \quad (5)$$

where  $k$  and  $n$  are constants.

The above relation models the experimental data very accurately and gives access to zero shear viscosities for higher polymer concentrations where direct measurements become difficult. The exponent  $n$  was found to vary between  $2/3$  and  $1/2$ . A common analysis of all data demonstrates the impossibility to construct a master curve by merely shifting the axis, in contrast to the situation encountered with systems for which shear thinning results from entanglements. This finding implies that the usual proportionality between the zero shear viscosities and the characteristic

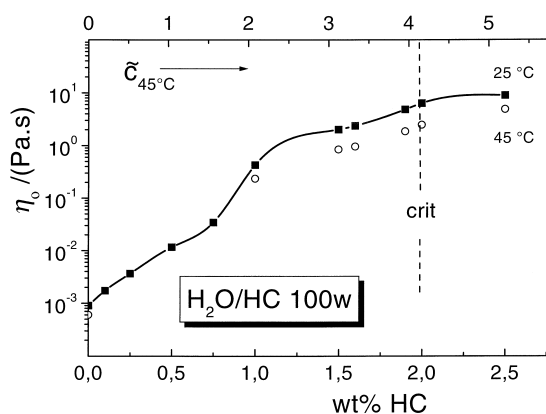


Fig. 7. Zero shear viscosity as a function of the weight fraction of HC for 25°C; some data for 45°C (open symbols) are also indicated. The upper abscissa gives the composition in terms of the degree of coil-overlap  $\bar{c} = c_2[\eta]$  at 45°C.

viscometric relaxation times [13] is lacking for the present system.

The above mentioned differences in the flow behaviour become plausible if one takes the unlike molecular mechanisms underlying shear thinning into consideration. For the present system, the observed reduction of  $\eta$  as  $\dot{\gamma}$  rises is attributed to a disruption of intersegmental clusters between favourably interacting parts of the polymer backbone (in particular between the hydrophobic entities) which are formed under equilibrium conditions and can be destroyed by sufficiently high shear rates. This assessment is backed by different types of investigations performed with copolymers. NMR experiments [14] have provided evidence for the existence of long-lived intersegmental clusters and shear influences [15] on the phase separation observed with homopolymer/copolymer blends could be explained theoretically [16] in terms of a destruction of the intersegmental clusters established in the stagnant systems (quasi-chemical equilibria). Along these lines the absence of a master curve becomes conceivable as a result of the complicated

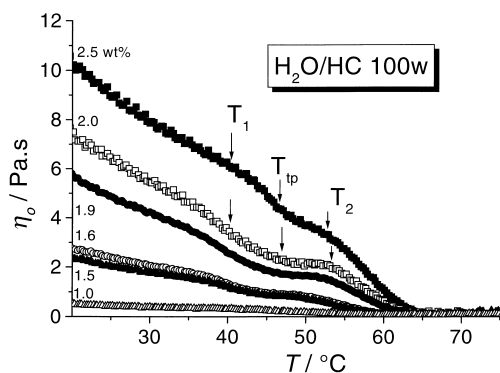


Fig. 8. Zero shear viscosity as a function of temperature for different weight fractions of HC. The arrows shown for the two highest polymer concentrations indicate  $T_1$  and  $T_2$  (cf. Fig. 2); also marked is  $T_{tp}$ , the lowest temperature at which two macroscopically coexisting phases can be observed in the quiescent state.

superposition of normal temperature effects and contributions of thermodynamically induced changes in the number and average life time of intersegmental clusters acting as temporary physical cross-links.

### 3.4. Zero shear viscosities

The influence of polymer concentration on  $\eta_0$  is shown in Fig. 7 for two temperatures; to ease discussion, compositions are also shown in terms of  $\bar{c} = c_2[\eta]$ , the degree of coil-overlap. For a given composition of the mixture,  $\bar{c}$  still varies via  $[\eta]$ , i.e. depends on temperature. For instance, at 25°C under favourable thermodynamic conditions one requires 2.3 mg of polymer to fill 1 ml of the solution with coils, whereas 11.3 mg are necessary at 55°C, where the solvent quality does no longer suffice to keep the mixture homogeneous over the entire range of composition and the isolated coils are much tinier.

At very low concentrations, in the region of pair interaction, the present system behaves normal, i.e. the limiting slope of  $\ln \eta$  versus  $c_2$  for high dilution is given by  $[\eta]$ . The extra contributions to  $\eta_0$ , superimposed to the general trend of  $\eta(w_{HC})$  in the composition range centred around  $\bar{c}_{45^\circ C} \approx 2$ , are attributed to the thermodynamic preference of different parts of the polymer chains leading to formation of soft, physically cross-linked microgels. The observation that the viscosity increase becomes less pronounced again as one approaches the critical composition is tentatively explained by the fact that these long-lived clusters increase in number and size so that they fill larger shares of the available volume. Under such circumstances the lower viscosity parts of a locally inhomogeneous system tend to dominate the dissipation of energy and to encapsulate the less readily flowing parts [17]. Such a situation should slow down the increase in  $\eta$  as the polymer concentration rises.

How the zero shear viscosity changes with temperature is demonstrated for different polymer concentrations in Fig. 8. Far from  $T_c$ , up to approximately 35°C, the behaviour is typical for polymer solutions and  $E^\ddagger$ , the activation energy of flow at constant shear rate, amounts to approximately 20 kJ/mol. At higher temperatures the solvent quality deteriorates considerably and the polymer coils shrink markedly as shown in Fig. 5 in terms of the intrinsic viscosities. This situation, plus the fact that intramolecular contributions gain importance over intermolecular ones, lead to a further reduction in  $\eta_0$ , which corresponds to higher  $E^\ddagger$  values ranging up to 70 kJ/mol. With the present system it is possible to perform reproducible measurements well into the two-phase regime. These data reveal an extra reduction in  $\eta$  which accelerates as the distance to the demixing temperature increases. In accord with the reasoning of the last section concerning the encapsulation of highly viscous parts of a locally inhomogeneous system it can be concluded that these data essentially refer to the less viscous coexisting matrix phase. For approximately critical compositions one observes an additional effect, namely an increase in

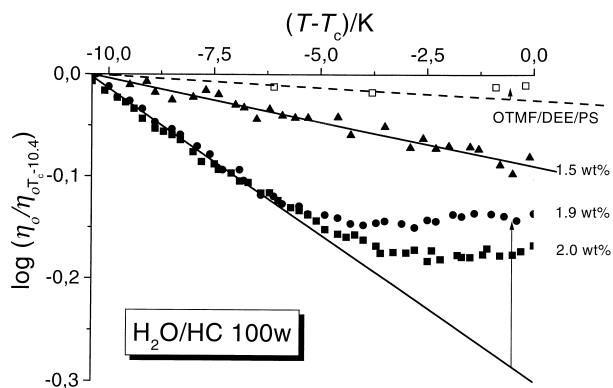


Fig. 9. Variation of the viscosity for aqueous solutions of HC of near-critical compositions with  $T-T_c$  the distance to the critical temperature for a given shear rate of  $1 \text{ s}^{-1}$ , normalized to the viscosity at  $T_c - 10.4$ . Also shown are literature data [18] for the critical composition of the system orthotrimethylformiate/acetone/polystyrene (215 kg/mol). Arrows indicate the effects resulting from critical fluctuations.

viscosity due to critical fluctuations. This phenomenon is discussed in more detail below.

### 3.5. Viscosity and phase separation

How the viscosity diminishes as one increases  $T$  and approaches the critical temperature can be seen from Fig. 9 for a constant shear rate of  $1 \text{ s}^{-1}$ . In order to make special effects resulting from the particular thermodynamic situation visible,  $\eta(T)$  is normalised to the viscosity observed at sufficient distance to  $T_c$  (in the present case 10.4 K) and plotted as a function of  $T - T_c$ . As a result of the small  $T$ -interval under consideration, Arrhenius behaviour corresponds in good approximation to straight lines.

The present evaluation demonstrates that the normal decrease in viscosity upon an increase in  $T$  comes to a halt in the case of near-critical composition of the solutions as the distance to  $T_c$  diminishes. This effect, which results from critical fluctuations can even lead to an increase in  $\eta$

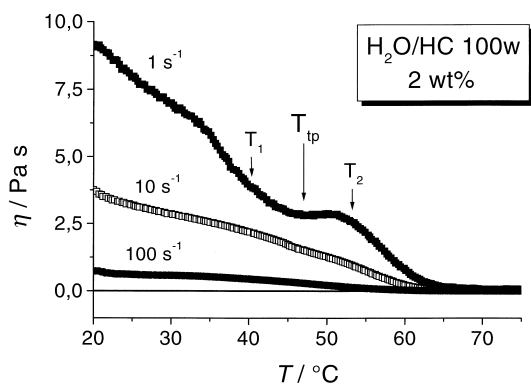


Fig. 10. Temperature dependence of the viscosity of a 2 wt.% aqueous solution of HC at different shear rates. The arrows indicate the  $T_1$  and  $T_2$  (cf. Fig. 2) values observed for the stagnant system; also marked is  $T_{tp}$ , the lowest temperature at which two macroscopically coexisting phases can be observed in the quiescent state.

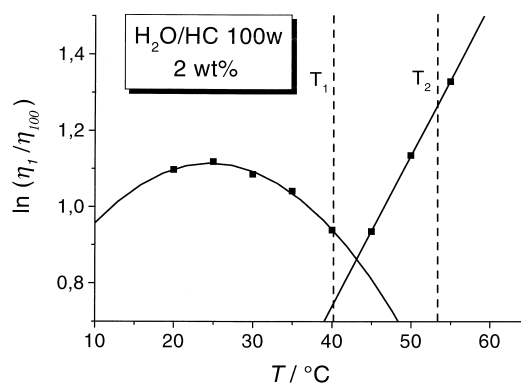


Fig. 11. Susceptibility of a 2 wt.% aqueous solution of HC towards shear thinning in terms of  $\eta_1/\eta_{100}$ , the ratio of the viscosities at  $1$  and  $100 \text{ s}^{-1}$ , read from Fig. 10, as a function of temperature. The discontinuity in the curve is interpreted as the segregation of a second phase.

upon an augmentation of  $T$ , as has been demonstrated for ordinary polymer/solvent systems exhibiting LCSTs [18]. With the aqueous solutions of HC of present interest, however, the effects are much more pronounced than usual as shown in Fig. 9. Very probably the occurrence of an uncommonly large thermodynamically induced extra dissipation of energy, indicated by arrows in this graph, can again be rationalized on the basis of long-lived intersegmental clusters. In terms of zero shear viscosities these critical contributions would be even more pronounced than for the present shear rate of  $1 \text{ s}^{-1}$ , where solutions of higher polymer concentration become already shear thinning as one approaches the critical temperature.

From the temperature dependence of the viscosity it is not only possible to notice precursors of the phases that coexist in the demixed state of the system via critical fluctuations but also the entrance into the two-phase regime as demonstrated by the following two graphs. At low shear rates the demixing temperature  $T_{tp}$  manifests itself as a minimum in  $\eta(T)$  (Fig. 10). The fact that this curve is rather flat does, however, not permit an exact viscometric determination of the phase separation conditions.

A common evaluation of the entire information obtained with a given solutions for different shear rates yields further and probably more precise evidence of demixing, as demonstrated for the data of Fig. 10. Taking  $\eta_1/\eta_{100}$ , the ratio of the viscosities at  $1$  and  $100 \text{ s}^{-1}$ , respectively, as a measure of the sensitivity towards shear thinning and plotting the logarithm of this value as a function of temperature yields the picture shown in Fig. 11.

The curve of the above graph falls into two clearly separable parts. Without further information it is hard to rationalize in detail why these branches look like they do. The increase in  $\eta_1/\eta_{100}$  as  $T$  is raised, starting from room temperature, is in agreement with the formation of larger intersegmental aggregates (deterioration of solvent quality) which can be destroyed by shear. Under these conditions  $\eta_1$  is identical with the zero shear viscosity and  $\eta_{100}$  moves deeper into the shear-thinning regime. For the reduction

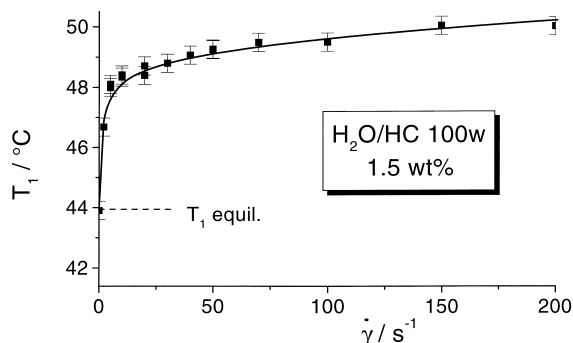


Fig. 12. Influence of shear rate on  $T_1$  (onset of turbidity, cf. Fig. 2) measured in the rheo-optical apparatus for a 1.5 wt.% aqueous solution of HC; also indicated is  $T_{1, \text{equil.}}$ , the value for the stagnant system.

observed as  $T$  is increased beyond 30°C the situation becomes more complex as not only  $\eta_{100}$  but also  $\eta_1$  are now located on the non-Newtonian part of the flow curve. The discontinuity upon surpassing the phase separation temperature is attributed to a change in the mechanism of shear thinning. On the high temperature side this effect is no longer due to the destruction of intersegmental clusters but to the deformation of the droplets of the suspended phase in the shear field [19]. This discontinuity in  $\ln \eta_1/\eta_{100}$  versus  $T$  should consequently offer a possibility to determine demixing temperatures. The fact that the thus obtained value results markedly lower than  $T_1$  measured for 100 s<sup>-1</sup> (cf. Fig. 12) at a comparable polymer concentration is in agreement with earlier findings according to which viscosity monitors changes in the phase state earlier than turbidity [20].

### 3.6. Shear influences on demixing

For ordinary polymer solutions it is well-established [5] that the phase separation of the flowing mixtures may differ considerably from equilibrium behaviour at shear rates above several hundred per second if the molar mass of the solute exceeds a few hundred kg/mol. In order to obtain some first information on the behaviour of the present system, orienting experiments were performed for a 1.5 wt.% solution of HC in water. The results shown in Fig. 12 indicate that the amphiphilic nature of this polymer again results in some peculiarities: despite its comparatively low molar mass one observes a pronounced extension of the homogeneous state by shear, even at shear rates below 2 s<sup>-1</sup>.

Again the destruction of intersegmental clusters (resulting from favourable interactions between the hydrophobic sites of the monomeric units) formed under equilibrium conditions by shear offers an explanation for this finding. This approach [16] dealing with the phase separation of flowing blends consisting of a homopolymer A and a random copolymer of A and B units, starts from the existence of long-lived B-cluster under equilibrium conditions. These entities can be destroyed by shear and lead to the

storage of energy in the flowing systems which modifies the Gibbs energy of mixing and consequently influences the phase separation behaviour. In this treatment of the phase separation of flowing systems as a near-equilibrium process the sign of shear effects depends on the curvature of the stored energy as a function of concentration [21]. Positive values lead to shear induced demixing and negative values to shear induced mixing. The already mentioned model calculation for copolymer blends yield positive curvatures for low concentrations of the cluster forming species. The expansion of the homogeneous state by shear observed for aqueous solutions of HC are for this reason in qualitative accord with that approach. Quantitative calculations are, however, required to check the validity of these considerations in more detail.

## 4. Conclusions

The phase diagram of the system H<sub>2</sub>O/HC 100w does not exhibit uncommon features. Due to the non-uniformity of the polymer, the critical point is shifted out of the minimum of the demixing curve towards higher polymer concentrations. Model calculations of the spinodal line and the measured temperature dependence of the intrinsic viscosity indicate slightly exothermal heats of mixing within the entire  $T$ -range. A comparison of  $T_{\text{tp}}$  (lowest temperatures for the macroscopic coexistence of two phases) with  $T_1$  (onset of turbidity) and  $T_2$  (fully developed turbidity) demonstrates that  $T_1$  is a good estimate of  $T_{\text{tp}}$  up to ca. 0.5 $w_c$  only, whereas  $T_{\text{tp}}$  is situated approximately half-way between  $T_1$  and  $T_2$  in the vicinity of the critical composition.

The rheological behaviour of aqueous solutions of HC 100w exhibits several particularities. Most obvious is the pronounced shear thinning despite the comparatively low molar mass of the polymer, even at high dilution and at low shear rates. This performance is attributed to long-lived intersegmental clusters (between the hydrophobic entities of the polymer backbone) forming under sufficiently unfavourable thermodynamic conditions in the quiescent state. As a result of the complex influences of temperature it turned out impossible to construct a master curve for  $\eta(T, \dot{\gamma})$ . The present system also exhibits some extra effects in the temperature and composition dependence of the zero shear viscosity. The effects can again be traced back to clusters that lead to temporary physical cross-links. These entities manifest themselves in an extraordinarily large excess viscosity, which—in the case of approximately critical composition—contribute up to 30% of the total viscosity as one approaches  $T_c$ . The segregation of a second phase can be seen rheologically in various ways. According to the present results the extent of shear thinning as a function of temperature monitors demixing best.

The last paragraph has briefly recalled how the thermodynamic situation influences the flow characteristics. Conversely flow does also induce changes in the phase

diagram. According to the present orienting experiments  $\dot{\gamma} \approx 50 \text{ s}^{-1}$  suffices to expand the homogeneous region by approximately  $5^\circ\text{C}$ . This finding can be rationalized—like all the other observations—in terms of intersegmental clusters. Their destruction by shear leads to the storage of energy in the flowing system and thus modifies the Gibbs energy of mixing.

### Acknowledgements

M.B. is grateful to the Alexander von Humboldt-Stiftung for a research fellowship; furthermore we would like to thank K. Thuresson, University of Lund, Sweden for drawing our attention to the present system and AKZO for supplying the polymer.

### References

- [1] Glass JE. Polymers in aqueous media: performance through association, *Adv Chem Ser*, 223. Washington, DC: American Chemical Society (ACS), 1989 chaps. 16–28.
- [2] Product Information, Akzo Nobel, Stenungsund, Sweden.
- [3] Thuresson K, Karlström G, Lindman B. *J Phys Chem* 1995;99:3823.
- [4] Enders S, Stammer A, Wolf BA. *Macromol Chem Phys* 1996;197:2961.
- [5] Krause C, Wolf BA. *Macromolecules* 1997;30:885.
- [6] Hiemenz PC. *Polymer chemistry: the basic concepts*. New York: Marcel Dekker, 1984.
- [7] Koningsveld R, Stavermann AJ. *J Polym Sci Part C: Symposia* 1972;31:345.
- [8] Flory PJ. *Principles of polymer chemistry*. Ithaca, NY: Cornell University Press, 1953.
- [9] Heskins M, Guillet JE. *J Macromol Sci Chem* 1968;A2:1441.
- [10] Schulz GV, Blaschke F. *J Prakt Chem* 1941;158:130.
- [11] Gundert F, Wolf BA. *J Chem Phys* 1987;87:6156.
- [12] Vinogradov GV, Malkin AY. *Rheology of polymers*. Moscow: Mir Publishers, 1980 Berlin: Springer.
- [13] Gerissen H, Gernandt F, Wolf BA. *Macromol Chem* 1991;192:165.
- [14] Fleischer G, Rittig F, Koňák Č. *J Polym Sci Part B: Polym Phys* 1998;36:2931.
- [15] Hinrichs A, Wolf BA. *Macromol Chem Phys* 1999;200:368.
- [16] Wolf BA. *J Chem Phys* 1999;110:7542.
- [17] Nielsen LE. *Polymer rheology*. New York: Marcel Dekker, 1977.
- [18] Breitenbach JW, Rigler JK, Wolf BA. *Angew Makromol Chem* 1977;57:15.
- [19] Lacroix C, Gramela M, Carreau PJ. *J Rheol* 1998;42:41.
- [20] Krämer-Lucas H, Schenck H, Wolf BA. *Makromol Chem* 1988;189:1613.
- [21] Wolf BA. *Macromolecules* 1984;17:615.